ELSEVIER

Int. J. Therm. Sci. 41 (2002) 261–267

International Journal of Thermal Sciences

www.elsevier.com/locate/ijts

A study of free convection in air around horizontal cylinders of different diameters based on holographic interferometry. Temperature field equations and heat transfer coefficients

J.V. Herráez *, R. Belda

Department of Thermodynamics, Faculty of Pharmacy, University of Valencia, 46100, Burjassot (Valencia), Spain

Received 29 May 2000; accepted 2 July 2001

Abstract

Holographic interferometry is used to study free convection in air around horizontal cylinders of different diameters and equal length, involving different surface temperatures, with the aim of defining the corresponding temperature fields. Interferograms were obtained to determine the temperature (T) of each point as well as its distance (x) from the surface of the cylinder. These values in turn made it possible to define functions (of an exponential nature in our case), $T = f(x)$, that satisfactorily reproduced the temperature fields. Posteriorly, these functions were used to calculate the local convection coefficients, determining their dependency upon temperature and the direction of measurement. Finally, the exponential functions were transformed into dimensionless expressions, and the corresponding Nusselt numbers were calculated for $Gr\,Pr$ product values of between 2.2×10^3 and 1.6×10^5.

Keywords: Free convection; Heat transfer; Local convection coefficient; Nusselt numbers; Holografic interferometry

1. Introduction

Engineering studies of free convection heat transfer from tubes or wires into an environmental fluid (generally air or water) require knowledge of the corresponding heat transfer coefficients. With the aim of contributing to the extensive literature on the subject, we have designed a study in which prior determination of the temperature fields surrounding the heating system is a fundamental element.

Many authors, including Sako [1], Chen and Yoon [2] and Farinas [3], have attempted to find theoretical solutions for such temperature fields, based on energy and movement conservation equations, while others have resorted to more traditional methods, fundamentally the positioning of thermometers in different regions of the field. However, an inconvenience of such approaches is that the thermometer tends to modify the field under study and moreover limits the investigation to point-by-point temperature assessments. Only the techniques employed by De Socio [4], or holographic interferometry—the performance of which has been extensively evaluated by Diez [7], Tokanai [8] and González [9], are able to afford a global assessment without altering the temperature field in the process.

The present study determines the temperature field around horizontal heating cylinders of equal length and different diameters, at different surface temperatures, that transmit heat to the surrounding air by free convection.

The determination of the distance of each interference line (isotherm) to the heated surface was used to obtain an exponential function of temperature as a function of distance for each radial direction of measurement. These functions were in turn used to calculate the local convection heat transfer coefficients.

Lastly, the corresponding local and mean Nusselt numbers were calculated as a function of the product $Gr\,Pr$.

2. Material and methods

2.1. Experimental design

Three heating cylinders with aluminum walls 0.105 m long and 0.001 m thick were used, with diameters of 0.01, 0.02 and 0.03 m. The cylinders were positioned horizontally

* Correspondence and reprints.
E-mail addresses: jose.v.herraez@uv.es (J.V. Herráez), rafael.belda-maximino@uv.es (R. Belda).

1290-0729/02/$ – see front matter
PII: S1290-0729(01)01314-X

Nomenclature

D	cylinder diameter	m	
Gr	Grashof number based on the cylinder diameter		
h_c	local convection coefficient	$W{\cdot}m^{-2}{\cdot}K^{-1}$	
k_f	thermal conductivity at $=(T_s+T_\infty)/2$	$W{\cdot}m^{-1}{\cdot}K^{-1}$	
L	cylinder length	m	
Nu	local Nusselt numbers		
Nu_m	average Nusselt numbers		
n_∞	air refraction index at infinity		
R	cylinder radius	m	
S	order of interference		
T	temperature	K	
T_S	temperature of the cylinder	K	
T_∞	temperature at infinity	K	
ΔT	temperature difference at $=(T_S-T_\infty)$	K	
$(dT/dx)_{x=0}$	thermal gradient in proximity to the wall	$K{\cdot}m^{-1}$	
x	distance along the cylinder	m	

Greek symbols

α	angular coordinate	rad
η	dimensionless distance	
λ	laser wavelenght	m
θ	dimensionless temperature	

in the air and were internally heated by identical electric resistances. The cylinder surface temperature was determined using chromel-constantan thermoelectric microcouples inserted symmetrically along the surface of the cylinder by means of the pinned-junction method. The entire experimental setup was placed on an antivibration table under conditions of pneumatic isolation, with prior erection of the optical setup required to obtain the interferograms via the double-exposure technique [7]. The interferograms were obtained in a plane perpendicular to the axis of each cylinder.

A total of 18 interferograms were obtained (6 for each cylinder of different diameter) at different cylinder surface temperatures in the range of 333–533 K. This temperature interval was chosen because values of under 333 K do not yield sufficient lines for valid fitting, while at above 533 K the interference lines are unable to afford measurements of sufficient resolution. This temperature interval provides $Gr\,Pr$ values in the range of 2.2×10^3 and 1.6×10^5.

2.2. Calculation of temperature and distance of the interference lines

Based on the interferograms obtained (three of which are shown in Fig. 1), we calculated the temperature (T) of each of the interference lines (isotherms), as well as the distance, x, to the surface of the cylinder in the 24 radial directions of measurement indicated in (Fig. 2).

2.3. Calculation of interference line temperature

The dark fringes appearing in the interferograms [6,7,9,12,13] correspond to destructive interference lines of the same temperature (i.e., isotherms). Their temperature was calculated as follows:

$$T = T_\infty/\left\{1-\lambda S/\left[L(n_\infty-1)\right]\right\} \tag{1}$$

in turn, $\lambda/[LT_\infty(n_\infty-1)]$ is constant and equal to $7.05\times10^{-5}\ K^{-1}$, and depends on the conditions of the experiment. The above equation thus becomes:

$$T = T_\infty/\left(1-7.05\times10^{-5}S\,T_\infty\right) \tag{2}$$

which is the equation used to calculate the temperature of each interference line (in each case involving a margin of error of 0.1 K).

2.4. Measurement of distance

The measurement of the distance, x, of each isotherm to the surface of the cylinder, in each of the directions of measurement, was carried out by projecting slides of the holograms onto a millimetered screen. The size of the resulting projected image was $2.4\times3.6\ m^2$, which allowed us to measure the corresponding distances with an error of 10^{-5} m. The results obtained in this way were more accurate than those calculated by densitometry.

The distributions of the temperatures and local convection coefficients are practically constant with respect to the angle α for values of α corresponding to the lower half (LH) of the plane, for evident reasons of symmetry of the interferograms; a mean value was therefore taken in the mentioned half plane, as shown in (Fig. 2).

The values of the distances used for fitting, in the upper half of the plane, correspond to the arithmetic mean of those obtained in the symmetrical directions with respect to the vertical axis (due to the previously mentioned symmetry reasons).

3. Results

3.1. Temperature field

The values corresponding to the temperatures and distances (x, T) obtained in each direction of measurement and for each of the 18 interferograms of the experiment generate

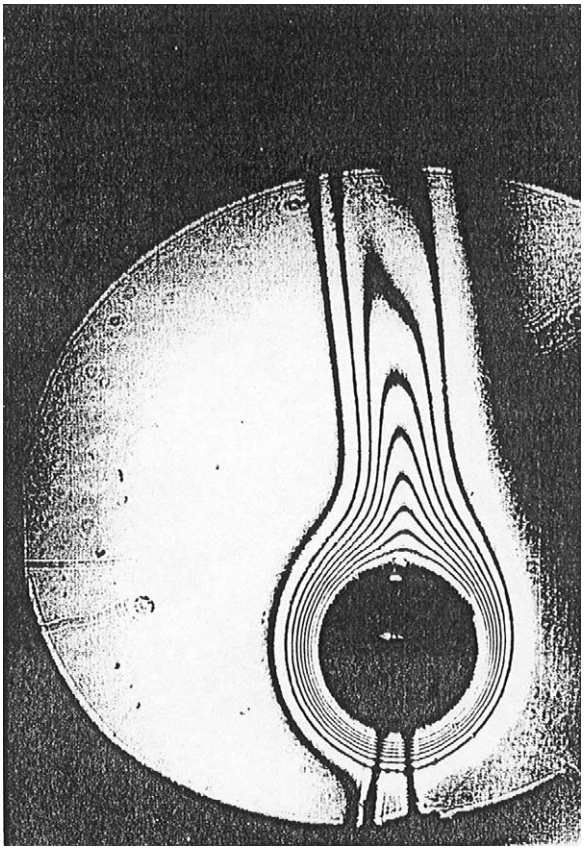

(a)

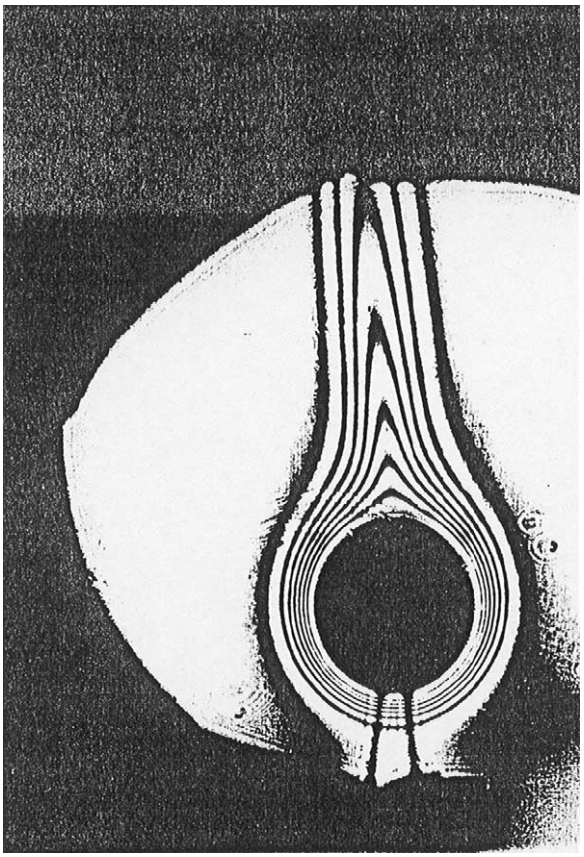

(b)

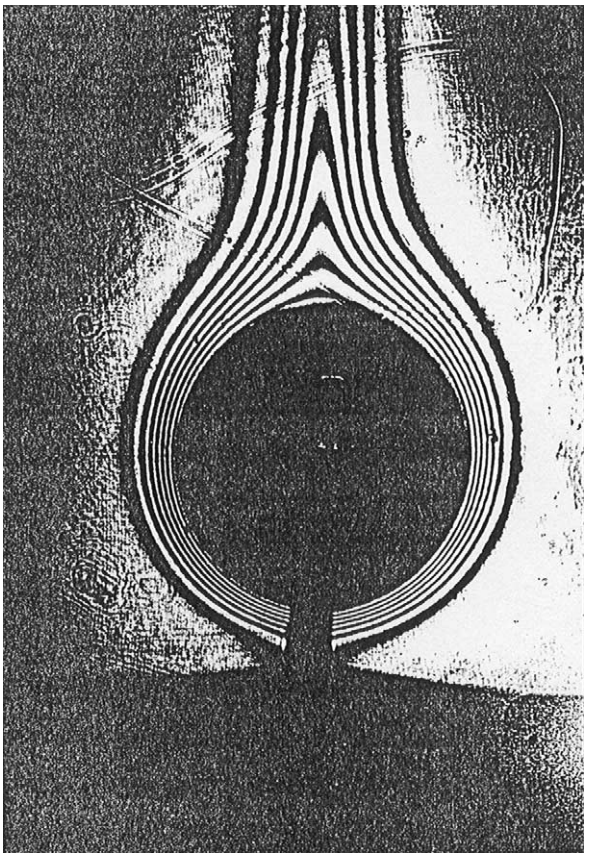

(c)

Fig. 1. Interferograms corresponding to a cylindrical tube 0.105 m in length, with respective diameters and surface and environmental temperatures of: (a) 0.01 m, 384.0 and 301.0 K; (b) 0.02 m, 349.5 and 298.4 K; (c) 0.03 m, 357.5 and 302.5 K.

a large volume of study data. As an example (Table 1) shows the data corresponding to one of these interferograms.

The values (x, T) corresponding to the above mentioned interferogram are reflected in (Fig. 3).

In all cases the experimental distributions could be fitted using exponential functions of the following type:

$$T = f(x) = T_\infty + (T_S - T_\infty) \cdot \mathrm{e}^{-kx} \tag{3}$$

which satisfies the limiting conditions that:

$T = T_\infty$ when $x \Rightarrow \infty$

$T = T_S$ when $x = 0$

with correlation coefficients that in all cases were >0.99, and which allowed us to calculate the value of k for each direction and interferogram. These functions constitute a novelty in this type of studies, and we believe that they afford a considerable advantage over the linear fits proposed by Hauff and Grigull [10]. In effect, while such linear fitting provides good results in proximity to the surface of the cylinder, and thus allows correct determination of the local convection coefficients, it is unable to adequately describe the temperature field at larger distances from the surface of the cylinder. In order to solve this problem, other

Table 1
Temperature and mean distance ($m \times 10^{-3}$) of each isotherm to the cylinder surface in the indicated measurement directions, for interferogram (b) in Fig. 1

Isotherm	$T(K)$	Angles (rad)									
		LH	$\pi/18$	$\pi/9$	$\pi/6$	$2\pi/9$	$5\pi/18$	$\pi/3$	$7\pi/18$	$4\pi/9$	$\pi/2$
1	345.3	0.16	0.17	0.17	0.17	0.18	0.20	0.26	0.36	0.68	1.72
2	337.1	0.62	0.69	0.69	0.70	0.73	0.76	0.84	1.23	2.49	6.56
3	329.4	1.02	1.08	1.09	1.10	1.12	1.38	1.68	2.51	4.16	11.12
4	322.0	1.71	1.71	1.69	1.71	1.75	1.89	2.26	3.50	6.88	17.10
5	314.9	2.50	2.49	2.49	2.51	2.72	2.91	3.60	5.47	9.93	26.48
6	308.1	3.51	3.64	3.65	3.69	3.77	4.10	5.52	7.69	14.17	–
7	301.6	5. 83	6.08	6.12	6.21	6.65	7.17	8.46	12.99	24.66	–

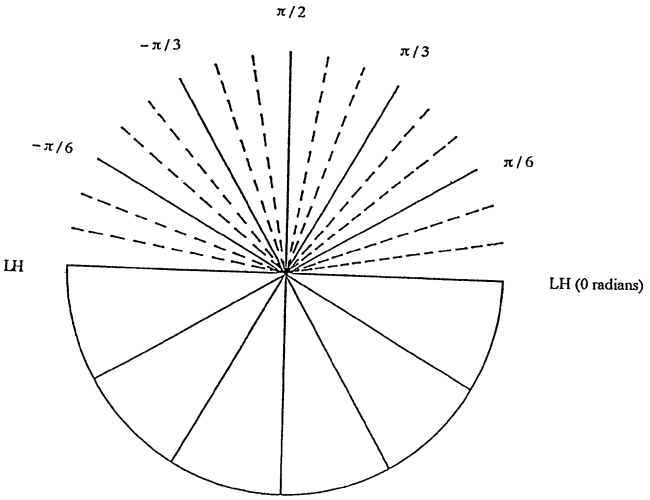

Fig. 2. Radial directions of measurement.

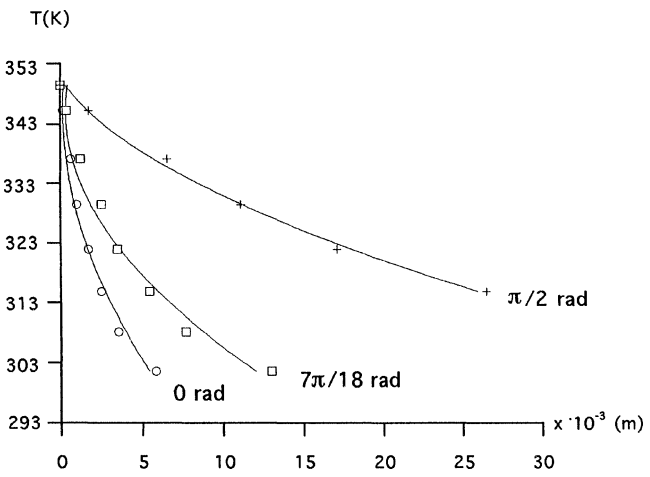

Fig. 3. Graphic representation of (x, T) in the directions indicated, for interferogram (b) in (Fig. 1).

authors such as Peterka and Richardson [15], and Anderson and Sounders [16], propose the use of polynomial functions that correctly describe the temperature field; however, since these generally fourth degree polynomial functions present five coefficients, the resulting polynomial expression affords an excellent correlation coefficient but without a stable tendency of the coefficients upon modifying the temperature or angle of measurement. These inconveniences are resolved by the experimental functions proposed in the present study, for in addition to offering excellent correlation coefficients in all cases, they imply a single coefficient that shows a stable tendency upon increasing temperature or modifying the angle of measurement, in addition to satisfying the limiting conditions of the experiment. As an example, (Table 2) shows the values corresponding to the interferograms depicted in (Fig. 1).

3.2. Local convection coefficients

Knowledge of the local convection coefficient, h_c, is clearly needed to calculate the heat transmitted by convection. In the most frequent case of natural convection (as in our experiment) in the zone close to the cylinder wall, it may be supposed that the fluid is either detained or displaces very slowly [14]; the so-called limiting layer theory can therefore be applied to calculate the corresponding h_c value in compliance with the hypothesis that heat transfer is preferentially the result of conduction. Based on this, we can apply the Fourier equation to the phenomenon:

$$dQ/s\,dt = k_f[dT/dx]_{x=0}$$

where $[dT/dx]_{x=0}$ is the thermal gradient close to the wall, and k_f is the thermal conductivity coefficient of air defined at the mean cylinder temperature, T_S, and room temperature, T_∞.

Taking into account that the heat transmitted to the fluid by this mechanism is to be transferred via convection to the rest of the fluid, we have:

$$dQ/s\,dt = -h_c(T_S - T_\infty)$$

from which by clearing h_c we obtain:

$$h_c = -k_f[dT/dx]_{x=0}/(T_S - T_\infty)$$

and considering the functions employed we have:

$$[dT/dx]_{x=0} = -k \cdot (T_S - T_\infty)$$

which leads to:

$$h_c = k \cdot k_f \tag{4}$$

This equation allows us to calculate the local convection heat transfer coefficients, for each direction of measurement.

Table 2
Values of k (m^{-1}) for the interferograms in Fig. 1, in the measurement directions indicated

Cylinder	Interferogram		Angles (rad)									
D (m)	$T_S(K)$	$T_\infty(K)$	LH	$\pi/18$	$\pi/9$	$\pi/6$	$2\pi/9$	$5\pi/18$	$\pi/3$	$7\pi/18$	$4\pi/9$	$\pi/2$
0.01	384.0	301.0	308	308	307	303	290	261	211	144	77	29
0.02	349.5	298.4	464	451	451	446	429	390	317	212	115	44
0.03	357.5	302.0	548	547	546	538	515	464	375	256	136	50

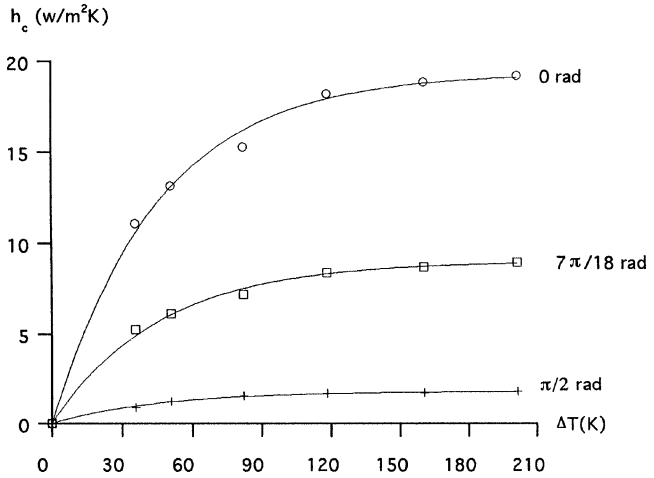

Fig. 4. Graphic representation of the local convection coefficients, h_c, as a function of the temperature difference $\Delta T = T_S - T_\infty$, for the cylinder of diameter 0.02 m, and for the directions indicated.

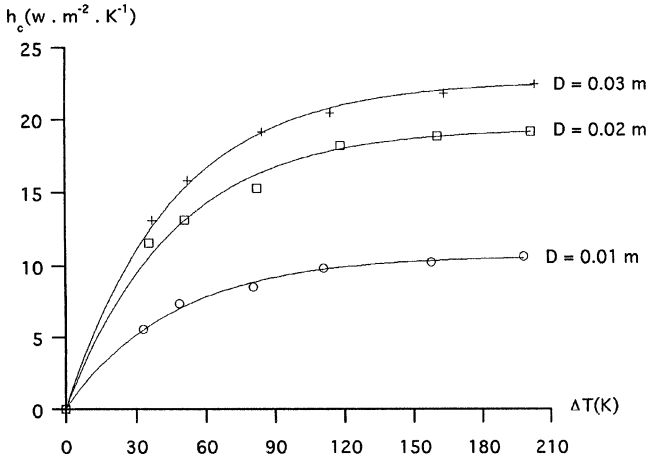

Fig. 5. Graphic representation of the local convection coefficients, h_c, as a function of the temperature difference $\Delta T = T_S - T_\infty$, for the cylinders of diameters 0.01, 0.02 and 0.03 m, in the 0 radians direction.

The h_c values thus obtained are represented as a function of the temperature difference, ΔT, between the heating cylinder and the surroundings, as reflected in (Fig. 4).

Likewise, and for comparative purposes, the values of h_c have been represented as a function of ΔT for a given direction, and for all three cylinder diameters considered (Fig. 5).

In the remaining directions increases in h_c similar to those presented were observed with increasing diameter.

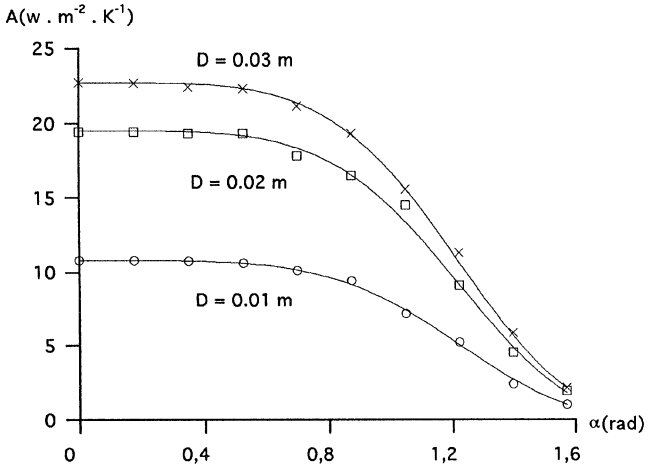

Fig. 6. Graphic representation of the values of the coefficient A, in (Eq. (5)), as a function of the radial directions of measurement, for each of the three cylinder diameters employed.

In all cases these distributions allowed fitting via functions of the following type:

$$h_c = A\left[1 - e^{-B\Delta T}\right] \tag{5}$$

which satisfactorily reproduce the experimental values of h_c for the temperature interval of our experiment, and with correlation coefficients of >0.99 in all cases, enabling us to calculate the coefficients A and B for each direction and series. In all fits coefficient B was seen to remain constant, with a value $B = 0.022\ K^{-1}$, and an error of less than 1%. In the case of coefficient A the corresponding error was less than 3% in all cases. The values obtained for A are shown in (Table 3).

On the other hand, we represented the values of coefficient A in Eq. (5), for each measurement direction and for each of the three cylinder diameters employed, as shown in (Fig. 6).

The points thus represented could be fitted by means of a function of the following type:

$$A = A_{\max} \cdot e\left[-M_1\alpha^{M_2}\right]$$

with correlation coefficients of >0.99 in all three cases.

In this expression $A_{\max}$ represents the maximum value of A, i.e., that corresponding to a measurement direction of 0 radians, and M_1 and M_2 are constants equal to 0.307 and 4.53, respectively. The above equation thus becomes:

$$A = A_{\max} \cdot e\left[-0.307\alpha^{4.53}\right] \tag{6}$$

Table 3
Values of A ($W{\cdot}m^{-2}{\cdot}K^{-1}$) for each series and measurement direction indicated

Cylinder D (m)	Angles (rad)									
	LH	$\pi/18$	$\pi/9$	$\pi/6$	$2\pi/9$	$5\pi/18$	$\pi/3$	$7\pi/18$	$4\pi/9$	$\pi/2$
0.01	10.79	10.79	10.76	10.69	10.12	9.14	7.57	5.04	2.68	1.00
0.02	19.45	19.45	19.40	19.22	18.31	16.48	13.70	9.09	4.83	1.81
0.03	22.72	22.72	22.66	22.50	21.39	19.25	16.14	10.62	5.64	2.12

3.3. Dimensionless temperature field

One way to generalize the results, eliminating the particularities of the experiment [1,14] is to convert the temperatures and distances to dimensionless values via the following transformations:

$$\theta = \left[(T - T_\infty)/(T_S - T_\infty)\right] \quad \text{and}$$

$$\eta = x \cdot \left(Gr^{1/4}/R\right)$$

Based on these transformations applied to (Eq. (3)), we can obtain functions of the following kind:

$$\theta = \mathrm{e}^{-k'\eta} \tag{7}$$

where:

$$k' = k \cdot \left(R/Gr^{1/4}\right)$$

which provides the dimensionless temperature field, with correlation coefficients of >0.99 in all cases; the corresponding graphic representations are omitted, for they are similar to those seen in (Fig. 3), with the corresponding change in scale.

3.4. Calculation of the Nusselt numbers (Nu)

By combining (Eq. (7)) and the Nusselt number of the diameter defined by:

$$Nu = (h_c D)/k_f = -\left(D[\mathrm{d}T/\mathrm{d}x]_{x=0}\right)/(T_S - T_\infty)$$

we obtain the following expression:

$$Nu = -2Gr^{1/4}(\mathrm{d}\theta/\mathrm{d}\eta)_{\eta=0}$$

Since in our experiment $(\mathrm{d}\theta/\mathrm{d}\eta)_{\eta=0} = -k'$, and considering that $k' = k \cdot (R/Gr^{1/4})$ substitution yields:

$$Nu = 2 \cdot k' \cdot Gr^{1/4} = 2 \cdot k \cdot R = k \cdot D \tag{8}$$

as a result of which the determination of k for each direction and temperature allows us to calculate the corresponding local Nusselt number.

To the effects of our experiment, these values can also be calculated by substituting (Eq. (5)) in the definition of the Nusselt numbers, thus obtaining the expression:

$$Nu = (h_c \cdot D)/k_f = A\left[1 - \mathrm{e}^{-0.022\Delta T}\right] \cdot D/k_f \tag{9}$$

This equation allowed us to calculate the local Nusselt numbers for each measurement direction at the temperatures involved in our study. Based on these values, by applying the mean value theorem, we obtained the corresponding mean Nusselt numbers (Nu_m) for each cylinder diameter and temperature of the experiment.

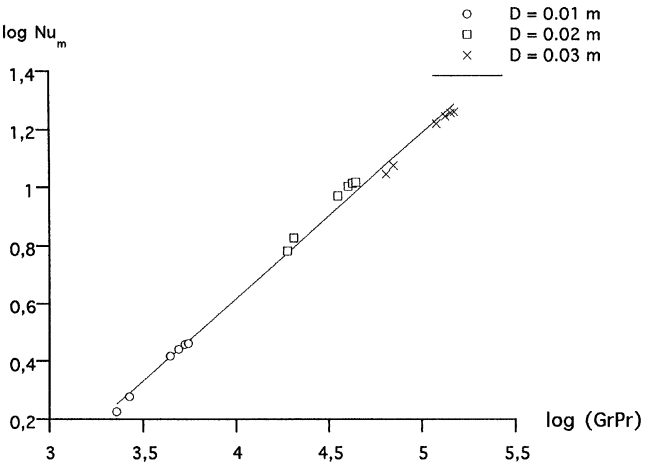

Fig. 7. Values of $A_{\max}$ as a function of cylinder diameter.

In this way we were able to represent log Nu_m versus log ($Gr\,Pr$), as shown in (Fig. 7).

The fitting function obtained, with a correlation coefficient >0.99, is expressed by the following equation:

$$Nu_m = C(Gr\,Pr)^m \tag{10}$$

where: $C = 0.022$ and $m = 0.5682$, thus allowing comparison of our results with the values published by Mc Adams [11].

In our case the values of log ($Gr\,Pr$) were between 3.34 and 5.20, showing that values of >4 afford acceptable agreement between our Nu_m values and those reported in the literature. However, for log($Gr\,Pr$) values of <4 (corresponding in our case to cylinders with $D = 0.01$ m), we obtain Nu_m values that are significantly lower than those obtained by Mc Adams.

4. Conclusions

(1) Eighteen interferograms were obtained for heated cylinders measuring 0.01, 0.02 and 0.03 m in diameter, which allowed us to obtain their surrounding temperature fields by means of equations of the following type:

$$T = f(x) = T_\infty + (T_S - T_\infty) \cdot \mathrm{e}^{-kx}$$

(2) The coefficient, k, allows us to obtain the corresponding values of the local heat transfer coefficients, h_c, in proximity to the cylinder and for each measurement direction, by means of the expression $h_c = k \cdot k_f$, where k_f is the con-

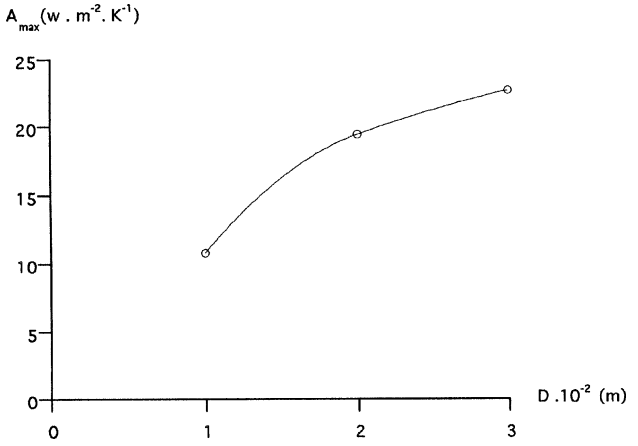

Fig. 8. Graphic representation of the values of the $\log Nu_m$, as a function of the valores of the $\log(Gr\,Pr)$, for the cylinders of diameters 0.01, 0.02 and 0.03 m.

ductivity coefficient of air at the mean temperature of the experiment.

(3) For each direction of measurement, we obtained expressions that provide the value of h_c as a function of $\Delta T = T_S - T_\infty$. Such expressions are of the type:

$$h_c = A\left[1 - e^{-0.022\Delta T}\right]$$

(4) The values of A depend upon the direction of measurement, the maximum value corresponding to the lower hemiplane LH (0 radians). For the rest of directions, the value can be obtained by the following expression:

$$A = A_{\max} \cdot e\left[-0.307\alpha^{4.53}\right]$$

(5) For one same direction with different cylinder diameters, the value of A is also seen to increase as shown in (Fig. 8), though the few points available do not allow us to derive a representative function.

(6) The Nusselt numbers corresponding to each direction of measurement can be obtained with the following expression:

$$Nu = k \cdot D$$

or alternatively:

$$Nu = A\left[1 - e^{-0.022\Delta T}\right] \cdot D/k_f$$

(7) The relation between Nu_m and the product $(Gr\,Pr)$ is given by:

$$Nu_m = 0.022(Gr\,Pr)^{0.5682}$$

References

[1] M.T. Sako, T. Chiva, J.M. Salinas, A. Yanagida, Numerical solution of transient natural convective heat transfer from a cylinder, Heat Transfer-Jan. Res. 11 (1982) 27–44.
[2] C.J. Chen, Y.H. Yoon, Finite analytical numerical solution axisymmetric Navier–Stokes and energy equations, J. Heat Transfer. 105 (1983) 18–29.
[3] M.I. Farinas, A. Garon, K. St Louis, Study of heat transfer in a horizontal cylinder with fins, Rev. Gén. Therm. 36 (5) (1997) 398–410.
[4] L.M. De Socio, Laminar free convection from a horizontal cylinder—parallel and flow regimens, Internat. J. Heat Mass Transfer 1 (1984) 15–27.
[5] E. Kaiser, Interferometrical temperature field measurement for a thermic fluid velocity sensor, M.S.R. 27 (4) (1984) 151–154.
[6] Z. Zemanet, Evaluation of a holographic interferogram of a two-dimensional temperature field in water, Jemma Mech. Opt. 29 (4) (1984) 109–112.
[7] R. Diez, M. Dolz, R. Belda, J.V. Herraez, M. Buendia, Free convection around a horizontal circular cylinder. Dimensionless empirical equations, Appl. Sci. Res. 46 (1989) 365–378.
[8] H. Tokanai, M. Kuriyama, E. Harada, H. Konno, Natural convection heat transfer from vertical and inclined arrays of horizontal cylinders to air, J. Chemical Engrg. Japan. 30 (4) (1997) 728–734.
[9] R. Gonzalez, P. Wintz, Digital Image Processing, Addison-Wesley, Reading, MA, 1987.
[10] W. Hauff, U. Grigull, Optical Methods in Heat Transfer. Advances in Heat Transfer, Academic Press, New York, 1970.
[11] W.H. Mc Adams, Trasmision de la chaleur, Dunad, Paris, 1964.
[12] S. Inada, T. Taguchi, W.J. Yang, Effects of vertical fins on local heat transfer performance in a horizontal fluid layer, Internat. J. Heat Mass Transfer. 42 (15) (1999) 2897–2903.
[13] G. Lucarini, F. Piazza, C. Morandi, A. Pierfederici, Automatic temperature mapping system based on holographic interferometry, Electron. Lett. 18 (14) (1982) 523–524.
[14] A. Fortier, Mecanique des fluides et transferts de chaleur et de masse par convection, Masson et Cie, Paris, 1975.
[15] J.A. Peterka, P.D. Richardson, Natural convection from a horizontal cylinder at moderate Grashof numbers, Internat. J. Heat Mass Transfer. 12 (1969) 749–752.
[16] J.T. Anderson, O.A. Saunders, Convection from an isolated heated horizontal cylinder rotating about its axis, Proc. Roy. Soc. London A 217 (1953) 16–22.